X-ray crystal structure of a metalled double-helix generated by infinite and consecutive C*–Ag^{I}–C* (C*: N^{1}-hexylcytosine) base pairs through argentophilic and hydrogen bond interactions

Angel Terrón,[a],* Blas Moreno-Vachiano,[a] Antonio Bauzá,[a] Angel García-Raso,[a] Juan Jesús Fiol,[a] Miquel Barceló-Oliver,[a] Elies Molins,[b] and Antonio Frontera,[a],*

Dedication ((optional))

Abstract: The synthesis of a metalled double-helix containing exclusively silver-mediated C*–C* base pairs is reported herein (C* = N^{1}hexylcytosine). Remarkably, it is the first crystal structure containing infinite and consecutive C*–Ag^{I}–C* base pairs that form a double helix. The Ag^{I} ion occupies the center between two C* residues with N(3)-Ag bond distances of 2.1 Å and short Ag^{I}-Ag^{I} distances (3.1 Å) suggesting an interesting argentophilic attraction as a stabilization source of the helical disposition. The solid state structure is further stabilized by metal-mediated base-pairs, hydrogen bonding and π-stacking interactions. Moreover, the angle N(3)-Ag-N(3) is almost linear in the [Ag(N^{1}hexylcytosine)$_2$]$^{+}$ motif and the bases are not coplanar thus generating a double strand helical aggregate in the solid state. The noncovalent and argentophilic interactions have been rationalized by means of DFT calculations.

Introduction

The metal-mediated base pairs in nucleic acids, where a metal plays the role of hydrogen in a recognition bond, are of great interest in the developing of new nanomaterials, three recent reviews with natural bases have been published.[1] An interesting and differentiating feature of the Ag^{+} ion is that it exclusively binds to bases instead to the backbone of DNA. In fact, Gwinn's group has proved that DNA structure is strongly stabilized by guanine silver(I) mediated base pairs.[2] Moreover, it has been demonstrated that cytosine–cytosine base pair mismatches bind Ag(I) ions with high specificity in DNA duplexes.[3] The number of related studies and applications, using also non-natural bases, has increased exponentially.[4-6] Among them, the NMR solved structure of three consecutive imidazol-silver-imidazol base pairs must be emphasized. They were inserted in the centre of a 17-mer duplex in a AT alternating palindromic sequence of a right handed B-DNA-like structure.[7] Furthermore, the thymine-Hg(II)-thymine in a duplex of a B-form double helix, has been also characterized by NMR spectroscopy.[8] Finally the crystal structure of a silver(I)-RNA hybrid duplex containing Watson-Crick like cytosine-silver(I)-cytosine metallo base pairs and a related NMR structural study in solution of a DNA duplex comprising cytosine-Ag(I)-cytosine base pairs[9,10] have been recently published paving the way to the structure-based design of nucleic acid-based nanodevices. Despite these facts, the number of well-known X-ray structures of metal–mediated base pairs models or metal complexes with nucleic acids is very scarce in the literature. For pyrimidinic bases, the complexes are limited to Ag(I),[9-12] Hg(II),[11-17] and Pt(II).[18,19] Finally, for Au(III) there is only one example with RNA where the metal links a guanine to a cytosine.[20]

The number of possible recognition patterns between bases, where at least two hydrogen bonds are present, is 28 (either for DNA or RNA bases).[21] These patterns include the canonical Watson-Crick, or Hoogsteen and Haschemeyer-Sobell pairings, but other mismatch interactions have also been proved. An interesting example is the cytosinium-cytosine interaction through a linear N(3)-H···N(3) hydrogen bond as shown by some of us[22] and others[23] using X-ray crystallography. In this manuscript we report the synthesis and X-ray characterization double strand helical aggregate characterized by C*-silver-C* linear interaction (C* = N^{1}-hexylcytosine) and also Ag^{I}-Ag^{I} argentophilic interactions. Both interactions serve as stabilization sources for the final helical disposition of the assembly in the solid state.[24]

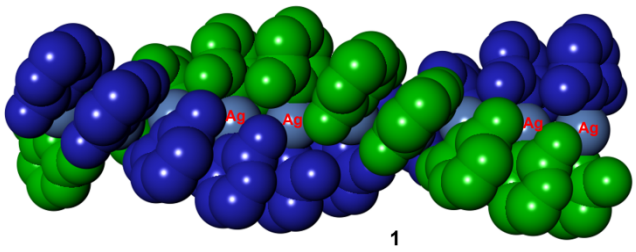

1

Figure 1. CPK representation double helix of **1**.

The helical form of the three-dimensional structure generated simply using N^{1}-hexylcytosine and Ag(I) metal ion (see Figure 1) provides significant foundation for structure-based design of metal-conjugated nucleic acid materials. DFT calculations are also reported to provide some physical insight

[a] Prof. Dr. A. Terrón,* Mr. B. Moreno-Vachiano, Mr A. Bauzá, Prof. Dr. A. García-Raso, Prof. Dr. J. J. Fiol, Prof. M. Barceló-Oliver and Prof. A. Frontera*
Department of Chemistry
Universitat de les Illes Balears
Crta. de Valldemossa km 7.5, 07122 Palma de Mallorca, Spain
E-mail: angel.terron@uib.es; toni.frontera@uib.es
[b] Prof. Dr. E. Molins
Institut de Ciència de Materials de Barcelona (ICMAB-CSIC),
Campus de la Universitat Autònoma de Barcelona, 08193
Bellaterra, Spain

Supporting information for this article is given via a link at the end of the document.((Please delete this text if not appropriate))

into the noncovalent H-bonding and argentophilic interactions. It should be mentioned that Lee *et al.*[25] have described the synthesis and characterization of simple 1:2 silver(I) pyridine adducts of different counter-anions, exhibiting strong ligand-unsupported argentophilic interactions between $[Ag(py)_2]+$ ions, forming dimers $[Ag(py)_2]_2^{2+}$. These dimers are further linked into 1-D infinite chains by a combination of Ag···Ag contacts, π–π stacking, and anion bridging interactions.[25] The main difference with the structure reported herein is that compound **1** forms a double strand helical aggregate in the solid state, apart from the different nature of the pyrimidine base. Another differentiating feature is the formation of hydrogen bonds and extended π–stacking interactions between the bases that synergistically stabilize the helical structure.

Table 1. Crystal data and structure refinement for **1** (CCDC 1496538).

	1
Empirical formula	$5(C_{20}H_{34}AgN_6O_2)\cdot5(SbF_6)\cdot2(CH_4O)$
Formula weight	3734.90
Temperature	183(2) K
Wavelength	0.71073
Crystal system	Monoclinic
Space group	P 21/n
Unit cell dimensions (Å,º)	a = 15.8289(4) b = 30.0084(7) c = 29.7058(8) β= 100.257(3)
Volume	13884.8(6)
Z	4
Density (calculated)	1.787 Mg/m^3
Absorption coefficient	1.749 mm^{-1}
F(000)	7424
Crystal size	0.355 x 0.272 x 0.165 mm^3
Theta range for data collection	2.259 to 22.464.
Index ranges	-26≤h≤27, -50≤k≤51, -47≤l≤49
Reflections collected	193982
Independent reflections	70061 [R(int) = 0.1011]
Completeness to θ = 25.242º	99.9 %
Refinement method	Full-matrix least-squares on F^2
Data / restraints / parameters	70061 / 4037 / 2981
Goodness-of-fit on F2	0.802
Final R indices [I>2sigma(I)]	R_1 = 0.1239, wR_2 = 0.2780
R indices (all data)	R_1 = 0.3012, wR_2 = 0.3979

The angle N(3)-Ag-N(3) is almost linear (angles about 170º) and the bases are not coplanar. In fact they are alternated in a propeller twist with dihedral angles near 79º between the planes of the cytosine rings (see Figures 2 and 3). Each cytosine base establishes a π–π stacking interaction with the next coordinated complex generating a helix where each two consecutive bases are in an antiparallel conformation.

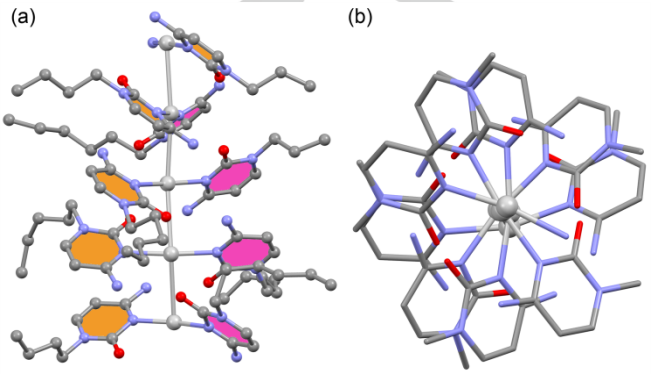

Figure 2. X-ray structure of the compound showing the helical structure, lateral and top view **1**. H-atoms omitted for clarity.

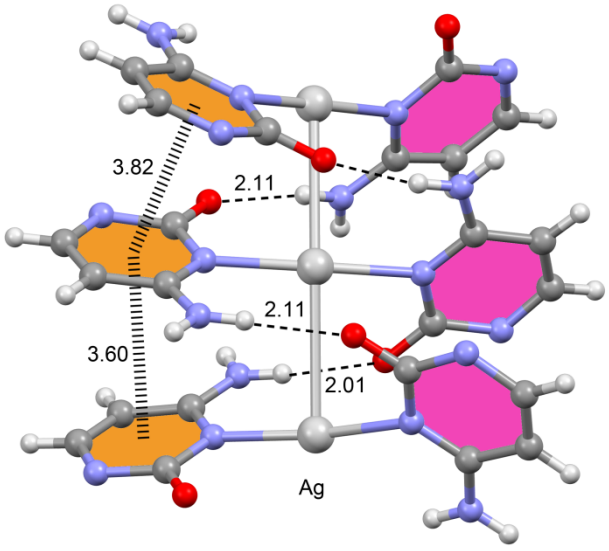

Figure 3. Base-base hydrogen-bonding pattern and π–stacking interactions found in the X–ray structure. Hexyl chains have been omitted for clarity. Distances in Å.

This π–π stacking interaction is important in the formation and stabilization of each individual strand. More importantly, the bases are linked through a hydrogen bond between an oxygen atom of the carbonyl group O(2) of one pyrimidine base and the amino group N(4) of the next adjacent complex motif, belonging to the two complementary helixes (Figure 3). This kind of

interaction has been postulated recently in solution CD studies.[26]

The N^1-hexyl chains present disorder and the alkyl–alkyl hydrophobic interactions likely contribute to stabilize the polymeric system. The counterions $[SbF_6]^-$ also present disorder and establish hydrogen bonding interactions with the alkyl chains. Both left and right handed double helixes are present in the solid state. Finally, two methanol molecules are allocated in the holes of each asymmetric unit. In the Figure 4 it is shown the unit cell of the X-ray structure that includes two right handed and two left handed helixes.

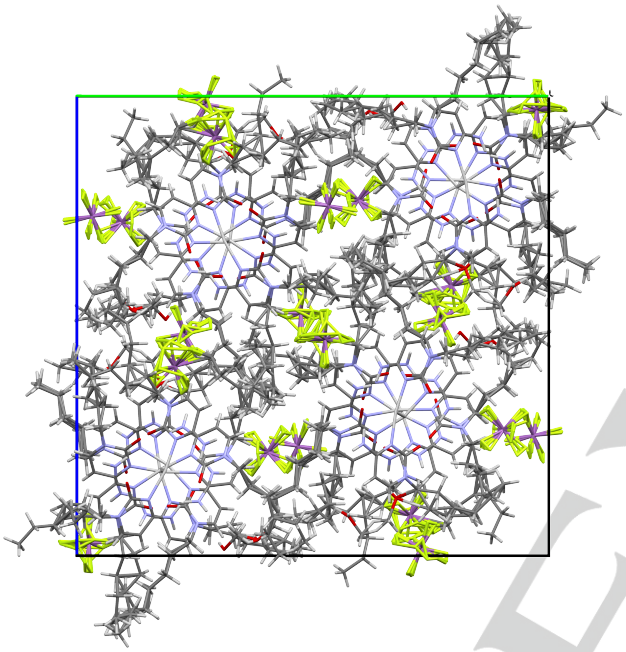

Figure 4. Cell packing along a axis, where four helixes, two right handed and two left handed, are shown.

In the polymeric structure the turn (when the bases are coincident through the projection of a axis) is made by 11 base pairs comprising two asymmetric units and eleven Ag ions (see Figure 5), similar to the turn of B-DNA (10.5 base pairs). Moreover, the on-top representation depicted in Figure 2b shows the typical pentagonal symmetry of the B-DNA.[29]

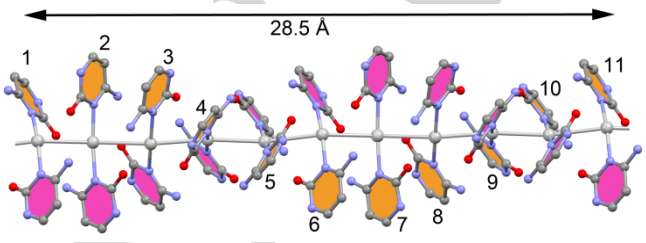

Figure 5. Partial view of the X-ray of **1**. Hexyl chains and H atoms omitted for clarity.

In comparison with other reported metalled double-helixes, this unprecedented model structure must be emphasized since it proves that Ag ions can promote the formation of double strand helical aggregate in the solid state without the presence of the sugar-phosphate backbone. Previous experiments as well as theoretical calculations indicated that guanine–silver–guanine base pair is more stable than that of cytosine–silver–cytosine[2] considering the bases coplanar. The hydrogen bond formation between the oxygen of one cytosine-motif with the amino group of the adjacent silver–cytosine motif in **1** can exist in other DNA-silver interactions and also in the silver(I)-RNA hybrid duplex reported by Ono and co-workers.[9] Another interesting feature of this double strand helical aggregate is the presence of an infinite sequence of $[Ag(N^1hexylcytosine)_2]^+$ motifs positively charged. Moreover, the successive Ag(I) metal ions forming an infinite 1D line may confer to this material interesting properties like one-dimension conductivity.

We have used DFT calculations (see theoretical methods) to further analyze the noncovalent interactions observed in the solid state of **1** that are crucial in the formation of the double helix. First of all, we have compared the interaction energies of several models of base pairs, which are shown in Figure 6. We have computed the *cis* Watson-Crick G–C* pair, *trans* C*–H^+C* and *trans* C*–Ag^+C* planar complexes (C* stands for N^1methylcytosine used as theoretical model of N^1hexylcytosine). Moreover, we have also computed an additional base pair using a modified cytosine [1-methylpyrimidin-2(1*H*)-one, denoted as C'], see Figure 6d. The interaction energy is larger in the C*–Ag^+C* (–59.4 kcal·mol^{-1}) pair than either the G–C* pair (–31.0 kcal·mol^{-1}) or the hemiprotonated C*–H^+C* pair (–48.5 kcal·mol^{-1}), confirming the affinity of Ag(I) to the N(3) atom of cytosine. To estimate the contribution of the H-bond in the planar C*–Ag^+C* pair, we have computed the interaction energy of the C'–Ag^+C' pair (H-bond not formed) which is –54.0 kcal·mol^{-1}. Consequently, the contribution of the H-bonds to the C*–Ag^+C* pair formation for the planar arrangement is –5.4 kcal·mol^{-1}.

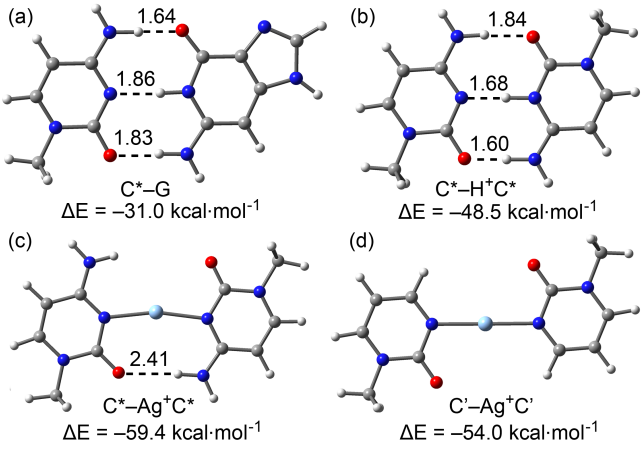

Figure 6. DFT optimized complexes and interaction energies of different base pairs (a-d). Distances in Å.

We have also computed a dimer extracted from the infinite double helix in order to compare the interaction energy of a non-planar $[C^*–Ag^+C^*]_2$ assembly with those shown in Figure 6. The geometry and interaction energy of the assembly is given in Figure 7. The interaction energy is very large (–107.7 kcal·mol^{-1}), almost twice the energy of the monomeric $C^*–Ag^+C^*$ pair. It should be emphasized the relevance of this large interaction energy, taking into consideration that a strong electrostatic repulsion is expected between both positively charged monomeric $[C^*–Ag^+C^*]$ units. We have computed an additional assembly $[C^*–Ag^+C']_2$ where two C* moieties have been replaced by C'. Consequently, the H-bonding interactions are not formed. As a result, the interaction energy is reduced to –94.7 kcal·mol^{-1} and, therefore, the contribution of the H-bonds in the helical structure is –13.0 kcal·mol^{-1}, considerably larger than the contribution in the planar $[C^*–Ag^+C^*]$ pair.

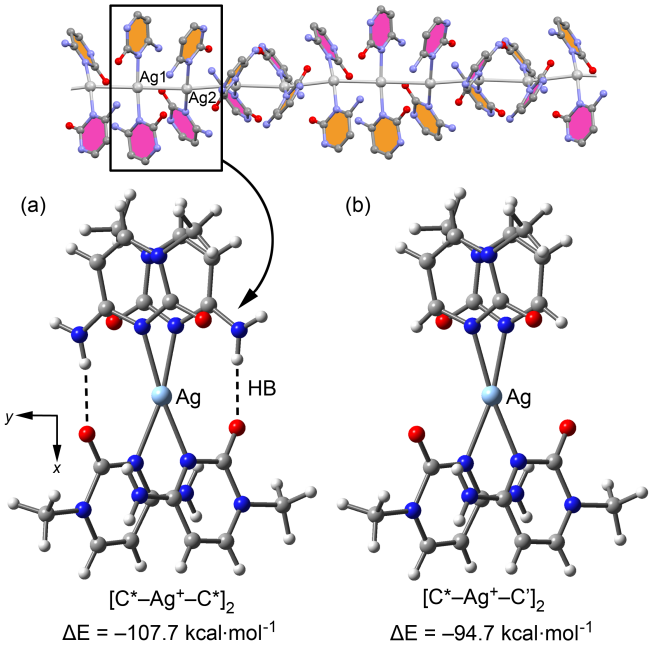

Figure 7. Interaction energies of a dimer (a) extracted from the polymeric double helix and a model without two NH_2 groups (b).

We have also performed the Bader's "atoms-in-molecules" analysis of the $[C^*–Ag^+C^*]_2$ dimer in order to characterize the interactions that contribute to the formation of the double helix. It is well established that the charge density ρ at the critical points (CPs) that emerge upon complexation gives helpful information regarding the strength of the noncovalent interactions involved in the complexes.[27] In Figure 8 we show the distribution of critical points and bond paths obtained from and AIM analysis. It can be observed a complicated distribution of critical points suggesting an intricate combination of several noncovalent forces that stabilize the assembly. The H-bonds are characterized by a bond CP that connects the H to the O atom of cytosine. Moreover, two O···Ag ancillary interactions are also present which are also characterized by a bond CP and bond path connecting O and Ag atoms. Interestingly, a bond path and bond CP connects both Ag ions confirming the existence of the Ag···Ag interaction. Moreover, the value of the Laplacian of the density at the bond CP that connect both Ag ions is positive revealing the closed shell nature of the argentophilic interaction. Finally, several bond ring and cage CPs characterize the π-stacking interaction of the cytosine rings.

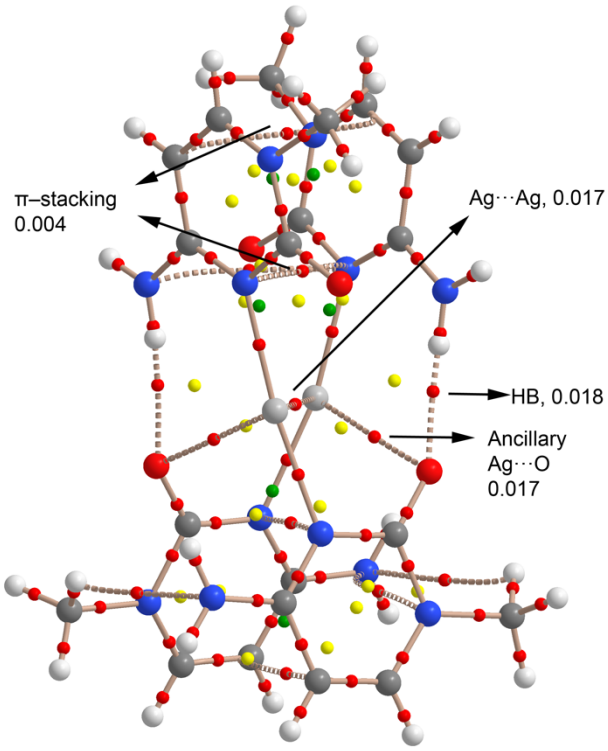

Figure 8. Distribution of critical points (CPs) in $[C^*–Ag^+C^*]_2$ dimer (bond CPs in red, ring CPs in yellow and cage CPs in green). The values of ·ρ for selected bond CPs are shown in a.u. The bond paths connecting the bond CPs are also represented.

Finally, we have studied the argentophilic interaction in the dimer shown in Figure 8a. This interaction is in principle counterintuitive, since it occurs against the Coulombic repulsion between two positively charged atoms. However, it has been demonstrated from a great deal of supramolecular structures[31] that Ag(I) centers are drawn together to ~3 Å, between the sum of van der Waals radii (3.44 Å) and the distance of a Ag–Ag single bond (2.53 Å). We have studied whether orbital contributions are important to explain the argentophilic interaction using Natural Bond Orbital (NBO) calculations. We have focused our attention on the second order perturbation analysis,[28] since it is very useful to study donor acceptor interactions.[28] For the $[C^*–Ag^+C^*]_2$ assembly we have found a relevant orbital contribution (–12.1 kcal/mol stabilization energy) due to an electron donation from the $4p_x$ of Ag(1) to empty $5d_{xy}$ orbital of Ag(2) (see Figure 6a for the axes orientation and Ag

labelling). Moreover, an energetically equivalent "retro-donation" $4p_x \rightarrow 5d_{xy}$ from Ag(2) to Ag(1) is also observed. Therefore the total stabilization energy due to donor-acceptor orbital interactions is $E^{(2)}$ = –24.2 kcal/mol, which is in good agreement with other calculations involving Ag dimers.[29]

Conclusions

In conclusion, we have synthesized and X-ray characterized the first crystal structure containing infinite and consecutive C*–Ag^{I}–C* base pairs. It presents a stunning helical structure where the Ag(I) metal center plays a prominent role inter-connecting the N^1hexylcytosine forming the C*–Ag^{I}–C* base pairs and simultaneously connecting those pairs by means of argentophilic interactions to yield the double strand helical aggregate. The most important interactions found in the structure have been characterized and analysed using DFT calculations. This investigation may open the door to the synthesis of Ag-cytosine nanomaterials and contribute to explain the formation mechanism of water soluble nanoclusters based on silver and cytidine.[30]

Experimental Section

Elemental microanalyses were carried out using a Carlo Erba model 1108 microanalyzer. **IR spectra** in the solid state (KBr pellets) were measured on a Bruker IFS 66 spectrometer. **NMR spectra** were recorded on a Bruker AMX300 spectrophotometer at room temperature. ^{1}H shifts in deuterated dimethyl sulfoxide (DMSO-d6) were referenced to DMSO-d6 [^{1}H-NMR, δ(DMSO) = 2.47 ppm; N1-hexylcytosine was obtained as described before.[21] Reagents were used as received from Sigma-Aldrich. **MALDI Mass spectra measurements** were performed on an Autoflex III MALDI-TOF/TOF mass spectrometer (Bruker Daltonics, Leipzig, Germany) equipped with a 200-Hz Smartbeam laser. Spectra were recorded in the reflector positive mode a within a mass range from 60 to 1000 Da. The IS1 voltage was 19 kV, the IS2 voltage was maintained at 16.70 kV, the lens voltage was 8.10 kV, *Reflector*= 21.00 kV, *Reflector* 2= 9.60 kV and the extraction delay time was 40 ns. The matrix used was a saturated solution of α-cyano-4-hydroxy-cinnamic acid in 50% acetonitrile-2.5% trifluoroacetic acid. 0.5 microliters of a proportion 50:10 (matrix:sample) were placed onto a spot of a ground steel target (Bruker Daltonics) and air dried at room temperature. For each spectrum were collected and analyzed approximately 500 shots from different positions of the target spot. The spectra were calibrated internally using PEG (Polyethylene glycol) 400.

Synthesis of $[Ag(N^1\text{-hexilcytoine})_2]_5(SbF_6)_5(CH_3OH)_2$

1 mmol of N^1-hexylcytosine[22] (195.14 mg) was dissolved in 25 cc of methanol. To this solution another one of ½ mmol of $AgSbF_6$ in 25 cc of methanol was added slowly with care that light don't affect. The mix was heated at reflux during 2 hours. The final solution was filtered out, when still it is warm, and let to stand to crystallize. Eight days later crystals appear. The white crystals with the appearance of bars were filtered with paper avoiding light. The yield in crystals is 33%.

^{1}H RMN (300 MHz, [D6]DMSO, 25º): δ = 7.91 (s, 2H, NH_2), 7.75 (d, 1H, CH, ^3J(H,H) = 7.2 Hz), 5.83 [d, 1H, CH, ^3J(H,H) = 6.9 Hz), 3.68 (t, 2H, CH_2, ^3J(H,H) = 7.2 Hz), 1.54 (m, 2H, CH_2), 1.22 (br s, 6H, 3xCH_2), 0.82 ppm (t, 3H, CH_3, ^3J(H,H) = 6.6 Hz); IR (KBr): 553vw, 446vw, 582w, 624w, 664 m, 711vw, 775m, 789w, 1115w, 1198m, 1269m, 1384s, 1440w, 1466w, 1490m, 1512s, 1619vs, 1665vs, 2857m, 2927m, 2957m, 3205m, 3351s cm^{-1}; MS (MALDI-TOF): $[C_{20}H_{34}AgN_6O_2]^+$ with a calculated exact mass of 497.1794, an experimental mass of 497.1789 was obtained with a minimal error of 3.5758 ppm (see Figure S1); elemental analysis calcd (%) for $C_{102}H_{178}Ag_5F_{30}N_{30}O_{12}Sb_5$: C 32.80, H 4.80, N 11.32; found: C 32.86, H 4.77, N 11.25.

X-ray diffraction details. Suitable crystals of **$[Ag(N^1\text{-hexilcytoine})_2]_5(SbF_6)_5(CH_3OH)_2$** were selected for X-ray single crystal diffraction experiments. Initial experiments were done mounting the selected crystal at the tip of a glass fibre on an Enraf–Nonius CAD4 diffractometer producing graphite monochromated Mo Kα radiation. After a random search of 25 reflections, the indexation procedure gave the cell parameters. Data were collected in the ω-2ϑ scan mode.

Looking for a better resolution of the crystal structure newly synthesized crystals were measured at low temperature in an Oxford Diffraction Xcalibur system with a CCD Ruby detector. Selected crystals were covered with oil (Infineum V8512, formerly known as Paratone N) and mounted at the tips of a glass fibre on the X-ray diffractometer. Crystallographic data was measured for three different crystals, at 183(2) K, using graphite monochromated Mo Kα radiation (λ = 0.7107 A). The program suite CRYSALISPro was used for data collection, anaytical absorption correction and data reduction.[31] Structure was solved with direct methods using SHELXL-2013[32] and was refined by full matrix least square method of F^2 with SHELXL-2013.

Non-H atoms were refined anisotropically and H-atoms were introduced in calculated positions and refined riding on their parent atoms. The aliphatic cues of the 10 cytosine moieties have been split over two complementary different positions in order to better model the natural mobility of this part. The compound also presents disorder on the SbF_6^- anions, which have been split in four different 25 % occupancy parts, each one. The occupancies of the disordered parts were allowed to freely refine until a constant number was obtained and then the values were changed by fixed ones in order to simplify the refinement job.

The structure presented in the paper corresponds to the best refined one, although the helicoidally positioned cytosine and silver complexes are equally disposed in all the studied crystals. All the information about X-ray refinement and the crystallographic coordinates of the final structure have been included in a separate supplementary file. The CCDC deposition number is 1496538.

Atomic Force Microscopy (AFM) was performed on a Atomic Forces Microscope *Multimode* with a controller *Nanoscope IV* de *Veeco.* The AFM tip is a silicon one, with a nominal curvature radium value of 10nm, and a nominal value for the forces constant of de 11.8 N/m. –the working mode was tapping in air. For the sample preparation, 60 ul of the mother solution were placed in a mica substrate during 35 minutes, the liquid was eliminated drying with a flux of nitrogen. More detailed information can be found in Supplementary Material.

Theoretical methods: The energies of all complexes included in this study were computed at the BP86-D3/def2-TZVP level of theory. The calculations have been performed by using the program TURBOMOLE version 7.0.[33] The interaction energies were calculated with correction for the basis set superposition error (BSSE) by using the Boys–Bernardi counterpoise technique.[34] For the calculations we have used the BP86 functional with the latest available correction for dispersion (D3).[35] The

NBO analysis has been perfomed at the BP86/def2TZVP level of theory by means of the Gaussian 09 calculation package.[36] The Bader's "Atoms in molecules" theory has been used to study the interactions discussed herein by means of the AIMall calculation package.[37]

Acknowledgements

The authors are indebted to B. Spingler and R.K.O. Sigel (University of Zürich) for the use of X-ray facilities. Financial help from the Govern de les Illes Balears, project number AAEE 38/2014 (Conselleria d'Educació, Cultura i Universitats and Feder Funds) and from Spanish Authorities DGICYT Project numbers CTQ2015-71211-REDT and CTQ2014-57393-C2-1-P, CONSOLIDER-Ingenio 2010 project CSD2010-0065 (FEDER funds) are also acknowledged.

Keywords: N1-hexylcytosine • Silver • Double helix • X-ray crystallography • DFT calculations

[1] a) D. A. Megger, N. Megger, J. Müller, *Met. Ions Life Sci.* **2012**, *10*, 295-317; b) B. Lippert, P.J. Sanz Miguel, *Acc. Chem. Res.* **2016**, *49*, 1537-1545; c) .T. Dairaku, K. Furuita, H. Sato, J. Šebera, K. Nakashima, A. Ono, V. Sychrovsky, C. Kojima, Y. Tanaka, *Inorg. Chim. Acta* **2016**, *452*, 34-42.

[2] S. M. Swasey, L. Espinosa-Leal, O. Lopez-Acevedo, J. Pavlovich, E. G. Gwinn, *Scientific Report*s **2015**, *5*, 1-9.

[3] A. Ono, S. Cao, H. Togashi, M. Tashiro, T. Fujimoto, T. Machinami, S. Oda, Y. Miyake, I. Okamoto, Y. Tanaka, et al. *Chem. Commun.* **2008**, 4825-4827.

[4] Y. Takezawa, M. Shionova, *Acc. Chem. Res*. **2012**, *45*, 2066-2076.

[5] G. H. Clever, C. Kaul, T. Carell, *Angew. Chem. Int. Ed*. **2007**, *46*, 6226-6236.

[6] T. Biver, *Coord. Chem. Rev.* **2013**, *257*, 2764-2783.

[7] S. Johansen, N. Megger, D. Boehme, R. K. O. Sigel, J. Müller, *Nat. Chem.* **2010**, *2,* 229-234.

[8] H. Yamagouchi, J. Sebera, J. Kondo, S. Oda, T. Komura, T. Kawamura, T. Dairaku, Y. Kondo, I. Okamoto, A. Ono, J. V. Burda, C. Kojima, V. Sychrovský, Y. Tanaka *Nucleic Acids Res*, **2014**, *42*, 4904-4909.

[9] J. Kondo, Y. Tada, T. Dairaku, H. Saneyoshi, Y. Okamoto, Y. Tanaka, A. Ono, *Angew. Chem. Int. Ed.* **2015**, *54*, 13323- 13326.

[10] T. Dairaku, K.Furuita, H. Sato, J. Šebera, K. Nakashima, J. Kondo, D. Yamanaka, Y. Kondo, I. Okamoto, A. Ono, V. Sychrovsky, C. Kojima, Y. Tanaka *Chem Eur. J*. **2016**, 22, 13028-13032.

[11] T. J. Kistenmacher, M. Rossi, L. G. Marzilli, *Inorg. Chem.* **1979**, *18*, 240-244.

[12] K. Aoki, W. Saenger, *Acta Cryst.* **1984**, *C40* 775-778.

[13] J. Kondo, T. Tamada, C. Hirose, I. Okamoto, Y. Tanaka, A. Ono, *Angew. Chem. Int. Ed.* **2014**, *53,* 2385-2388.

[14] L. D. Kosturko, C. Folzer, R. F. Stewart, *Biochemistry* **1974**, *13*, 3949-3952.

[15] A. Bauzá, A. Terron, M. Barceló-Oliver, A. García-Raso, A. Frontera, *Inorg. Chim. Acta*, **2016**, *452*, 244-250.

[16] F. Zamora, K. Kunsman, M. Sabat, B. Lippert, *Inorg. Chem.* **1997**, *36,* 1583-1587.

[17] C. Y. Xu, F. Yu, L. H. Wang, Y. Zhao, T. Lin, C. H. Fan, J. H. He, PDB ID: 4R6M DOI: 10.2210/pdb4r6m/pdb.

[18] A. Erxleben, S. Metzger, J. F. Britten, C. J. L. Lock, A. Albinati, A. Lippert, *Inorg. Chim. Acta*, **2002**, *339*, 461- 469.

[19] M. S. Luth, M. Willerman, B. Lippert, *Chem. Commun* **2001**, 2058-2059.

[20] E. Ennifar, P. Walter, P. A. Dumas, *Nucleic Ac. Res.* **2003**, *32*, 2671-2682.

[21] I. Tinoko Jr in RNA World, R. F. Gesteland, J. F. Atkins (eds) Cold Spring Harboor Laboratory press (1993) Appendix I pp 603-607.

[22] M. Barceló-Oliver, B. A. Baquero, A. Bauzá, A. García-Raso, A. Terron, I. Mata, E. Molins, A. Frontera, *CrystEngComm* **2012**, *14*, 5777-5784.

[23] A. Schimanski, E. Freiseinger, A. Erxleben, B. Lippert, *Inorg. Chim. Acta* **1998**, *283*, 223-232.

[24] A. Terrón, B. Moreno-Vachiano, A. García-Raso, J. J. Fiol, M. Barceló-Oliver, E. Molins, in *Functional Metal Complexes that Bind to Biomolecules, Book of Abstracts of the 4th Whole Action Meeting of the COST Action CM1105*, (Eds.: M. Barceló-Oliver, J. Palou-Mir), ISBN 978-84-608-7064-7, Mallorca, **2016**, p. 111.

[25] C. Y. Chen, J. Y. Zeng, H. M. Lee, *Inorg. Chim. Acta* **2007**, *360*, 21-30.

[26] L. A. Espinosa Leal, A. Karpenko, A. Swasey, E. G. Gwinn, V. Rojas-Cervellera, C. Rovira, O. Lopez-Acevedo, *J. Phys. Chem. Lett.* **2015**, *6*, 4061-4066.

[27] R. F. W. Bader, *J. Phys. Chem. A* **2010**, *114*, 7431-7444

[28] F. Weinhold, C. R. Landis, Valency and Bonding: A Natural Bond Orbital Donor–Acceptor Perspective, Cambridge University Press, Cambridge UK, 2005.

[29] B. Pinter, L. Broeckaert, J. Turek, A. Ruzicka, F. De Proft, *Chem. Eur. J.* **2014**, *20*, 734-744.

[30] Y. Zhang, H. Jiang, W. Ge, Q. Li, X. Wang, *Langmuir* **2014**, *30*, 10910-10917.

[31] Oxford Diffraction Ltd., CRYSALISPro Software System, edition 1.171.37.31 (release 14-01-2014 CrysAlis171 .NET) (compiled Jan 14 2014,18:38:05), Oxford, UK.

[32] G. M. Sheldrick, *Acta Crystallogr.* **2008**, *A64*, 112–122.

[33] R. Ahlrichs, M. Bär, M. Hacer, H. Horn, C. Kömel, *Chem. Phys. Lett.*, **1989**, *162*, 165–169.

[34] S. B. Boys, F. Bernardi, *Mol. Phys.*, **1970**, *19*, 553–566.

[35] S. Grimme, J. Antony, S. Ehrlich, H. Krieg, *J. Chem. Phys.*, **2010**, *132*, 154104–154119.

[36] Gaussian 09, Revision **B.01**, M. J. Frisch, G. W. Trucks, H. B. Schlegel, G. E. Scuseria, M. A. Robb, J. R. Cheeseman, G. Scalmani, V. Barone, B. Mennucci, G. A. Petersson, H. Nakatsuji, M. Caricato, X. Li, H. P. Hratchian, A. F. Izmaylov, J. Bloino, G. Zheng, J. L. Sonnenberg, M. Hada, M. Ehara, K. Toyota, R. Fukuda, J. Hasegawa, M. Ishida, T. Nakajima, Y. Honda, O. Kitao, H. Nakai, T. Vreven, J. A. Montgomery, Jr., J. E. Peralta, F. Ogliaro, M. Bearpark, J. J. Heyd, E. Brothers, K. N. Kudin, V. N. Staroverov, R. Kobayashi, J. Normand, K. Raghavachari, A. Rendell, J. C. Burant, S. S. Iyengar, J. Tomasi, M. Cossi, N. Rega, J. M. Millam, M. Klene, J. E. Knox, J. B. Cross, V. Bakken, C. Adamo, J. Jaramillo, R. Gomperts, R. E. Stratmann, O. Yazyev, A. J. Austin, R. Cammi, C. Pomelli, J. W. Ochterski, R. L. Martin, K. Morokuma, V. G. Zakrzewski, G. A. Voth, P. Salvador, J. J. Dannenberg, S. Dapprich, A. D. Daniels, Ö. Farkas, J. B. Foresman, J. V. Ortiz, J. Cioslowski, and D. J. Fox, Gaussian, Inc., Wallingford CT, 2009.

[37] AIMAll (Version 13.05.06), Todd A. Keith, TK Gristmill Software, Overland Park KS, USA, 2013.

Entry for the Table of Contents

FULL PAPER

The synthesis and X-ray characterization of a metalled double-helix constructed by silver-mediated C–C base pairs is reported herein. Remarkably, it is the first crystal structure containing infinite and consecutive C–Ag^{I}–C base pairs. The Ag^{I} ion occupies the center between two C residues with N(3)-Ag bond distances of 2.1 Å and short Ag^{I}-Ag^{I} distances (3.1 Å) suggesting an interesting argentophilic attraction.

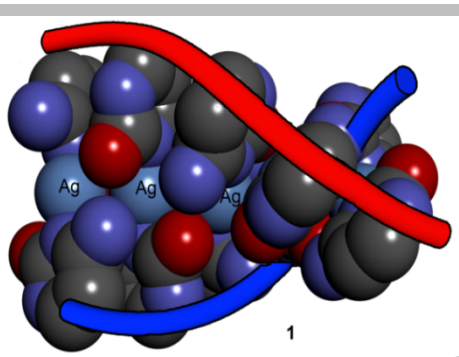

1

A. Terrón, B. Moreno-Vachiano, A. Bauzá, A. García-Raso, J. J. Fiol, M. Barceló-Oliver, E. Molins and A. Frontera**

Page No. – Page No.

X-ray crystal structure of a metalled double-helix generated by infinite and consecutive C*–Ag^{I}–C* (C*: N^{1}-hexylcytosine) base pairs through argentophilic and hydrogen bond interactions